Bionspired slippery surfaces by cluster-like ZnO@Co$_3$O$_4$ and its anti-corrosion performance

S. Gao[a,b], X. D. Li[a*], M. Zhang[a]
aSchool of Mechanical Engineering, Changchun University of Technology, Changchun, China,130012
b Department of Mechanical Engineering, College of Humanities&Information Changchun University of Technology, Changchun, China,130012

Herein, the super slippery surface composed of cluster-like ZnO@Co$_3$O$_4$ was prepared on the surface of Al alloy by a hydrothermal method. The morphology and composition of the film were characterized by SEM, XRD and XPS. In addition, electrochemical measurement results show that the impedance modulus at low frequency of cluster-like ZnO@Co$_3$O$_4$ SLIPS coatings was 6 orders of magnitude higher than that of the blank sample, and still 3 orders of magnitude towered over even after 28 days of immersion, which proves that the good storage capacity and long-term corrosion resistance.

1. Introduction

Metals and their alloys are the core engineering materials in many industrial fields. aluminum, copper, magnesium, steel and their alloys are common metals widely used in industrial, architectural, marine and aviation applications [1-3]. Aluminum is the most widely used metal material in nonferrous metals [4]. Aluminum products have a wide variety and are widely used in all sectors of the national economy [5,6]. Because aluminum alloy has a series of excellent physical, chemical, mechanical and processing properties, it can meet the various requirements for aluminum alloy materials from kitchen and tableware to cutting-edge technology, from building decoration industry to transportation industry, and from power system transmission cable application to aerospace different requirements [7-9]. However, aluminum and its alloys are prone to corrosion in seawater with Cl$^-$ and other special environments, and the surface is easy to freeze in extreme weather, which brings some difficulties and disadvantages to the wide use of aluminum and its alloys [10]. Therefore, how to improve the corrosion resistance of aluminum alloy in seawater and other media has always been one of the important research topics about aluminum and aluminum alloy.

At present, surface treatment is an effective protective measure against the defects of aluminum and its alloy surface in terms of corrosion performance. The industrialized surface protection treatment technology of aluminum alloy is most widely used in chemical conversion, anodizing, electroplating, electroless plating and organic polymer coating treatment [11-13]. The

---

chemical oxidation method uses chromate, phosphorus chromate and other treatments, but in order to eliminate the harmful impact of hexavalent chromium on the environment, it is necessary to carry out chromium free chemical conversion treatment [14]. Anodic oxidation is a process in which aluminum or aluminum alloy is used as anode to form porous oxide film on its surface. The oxide film can be colored. In order to meet the requirements of corrosion resistance, the porous film is usually sealed to obtain different functionality and decoration. However, this method will no longer be applicable when aluminum is in the marine atmosphere. For the study of corrosion resistance, anti-icing and self-cleaning of aluminum and its alloy surfaces, most of the protective organic coating measures are adding corrosion inhibitor and coating. However, these protective measures have some disadvantages, such as environmental pollution, complex process and so on.

Since Wenzel began to study the wettability of rough surfaces, people began to study superhydrophobic surfaces, but what really attracted people's attention was after professor Barthlott unveiled the mystery of superhydrophobic properties of lotus leaf surfaces in the late 1990s [15]. In the past 20 years, the research on superhydrophobic surfaces has made great progress both in theory and preparation technology. Because superhydrophobic surface materials show good corrosion resistance, anti-icing, self-cleaning and other characteristics, and due to the excellent physicochemical properties of aluminum and aluminum alloy materials, it has attracted extensive attention to make the aluminum alloy surface have superhydrophobic properties, so as to improve its corrosion resistance properties. However, superhydrophobic surfaces have multiple weaknesses, a low mechanical stability, low transparency and weak pressure stability [16]. Aizenberg et al. proposed a new type of slippery liquid-infused porous surface (SLIPS) material that was inspired by the Nepenthes pitcher plant which solve the problems of traditional lotus-leaf-inspired materials [17]. On the one hand, a protective barrier can be built on the metal surface to block the contact between aluminum alloy and corrosive medium; On the other hand, it fills the gap of superhydrophobic surface to improve the stability of the coating.

In this paper, a novel SLIPS with a cluster-like $ZnO@Co_3O_4$ structure was synthesized on an aluminium alloy. The surface has all the properties of a SLIPS, repelling all simple and complex liquids including water, milk, coffee, juice, ink, and others. The surface morphology, microstructure, surface chemical structure and chemical composition of the constructed aluminum alloy super sliding surface were characterized and analyzed by SEM, XRD and XPS. The corrosion resistance of the aluminum alloy super sliding surface was measured by electrochemical test, and the corrosion resistance and stability were discussed by simulated seawater immersion method. This provides potential application prospects for aluminum alloy corrosion protection.

2. Materials and methods

2.1. Materials

$Zn(NO_3)_2 \cdot 6H_2O$, $Co(NO_3)_2 \cdot 6H_2O$, NH_4F, urea, heptadecafluoro-1,1,2,2-tetradecyltrimethoxysilane, ammonium hydroxide ($NH_3 \cdot H_2O$, 25 wt%), and absolute ethanol were obtained from Aladdin Reagent Corp. (China); The DuPont Krytox 104 lubricant (PFPE) was purchased from America DuPont Krytox. The Al alloy substrates were purchased from Tianjin Guangfu Fine Chemical Research Institute. And the chemical composition shown in Table 1.

Table 1. Al alloy composition.

Component element	Al	Cu	Fe	Si	N
alloy composition（wt.%）	99.5	0.015	0.005	0.15	0.005

2.2. Method

2.2.1. Synthesis of ZnO@Co₃O₄ structure on Al alloy

The Al alloy substrates were abraded by with #600#, #1000# and #2000# sandpapers to remove the surface stain and oxide/hydroxide layer. Then, the alloys were ultrasonically cleaned in ethanol and deionized water for 5 min successively. Subsequently, 0.594 g of $Zn(NO_3)_2 \cdot 6H_2O$, 0.96 g of urea and 0.873 g of $Co(NO_3)_2 \cdot 6H_2O$ were dissolved in 30 mL of deionized water and stirred for 30 min. Next, 0.296 g of NH_4F was added and stirred for 10 min. The pretreated Al alloy and the above solution were transferred to the reaction vessel, kept at 120 °C for 5 h. Finally, the Al alloys were calcined at 360 °C for 1 h.

2.2.2. Synthesis of the cluster-like ZnO@Co₃O₄ SLIPS

10 μL of heptadecafluoro-1,1,2,2-tetradecyltrimethoxysilane and 50 ml of absolute ethanol was mechanically stirred for 2 h. Al alloy coated with the cluster-like $ZnO@Co_3O_4$ structure was immersed into the mixed solution for 2 h. Next, the as-prepared samples were immersed in DuPont Krytox 104 lubricant oil for 60 min, and then placed vertically for 12 h to removed excess oil to obtain the slippery liquid-infused surfaces.

2.2.3. Characterizations

The surface morphology was determined by SEM, using a JEOL JSM-6480A. Transmission electron microscopy (TEM, JEOL JEM 2100) micrographs obtained at a beam acceleration of 200 kV. The X-ray photoelectron spectroscopy (XPS, Thermo Scientific Escalab Xi+) experiments were performed. X-ray diffraction analysis (XRD, Rigaku TTR-III) was conducted with Cu Kα radiation at a wavelength of 0.15406 nm. The corrosion resistance was measured by electrochemical impedance spectroscopy (EIS, Zahner IM6, Germany) using a 3.5 wt% NaCl aqueous solutions at room temperature, and the experimental results were fit by ZSimpWin. The static contact angles and sliding angles were measured on a Data Physics OCA20 analysis system at room temperature.

3. Results and discussion

Figure 1 shows the SEM images of $ZnO@Co_3O_4$. It can be seen that the structure is cluster-like, which is composed of a large number of nanowires, including micron structure and nanostructure, with large specific surface area and voids. We know that the ''lotus leaf'' bionic superhydrophobic materials use the micro-nano structure to capture air to reduce the contact between the corrosive medium and the metal substrate. The reason why the superhydrophobic surface will fail is that the air in the micro-nano structure will escape under the action of pressure during the application process. Lubricant will replace air to fill the gap of micro-nano structure of $ZnO@Co_3O_4$. It provides favorable conditions for the storage of lubricating fluid and can obtain an ideal super slippery surface. In addition, this structure can also effectively prevent the loss of lubricating fluid
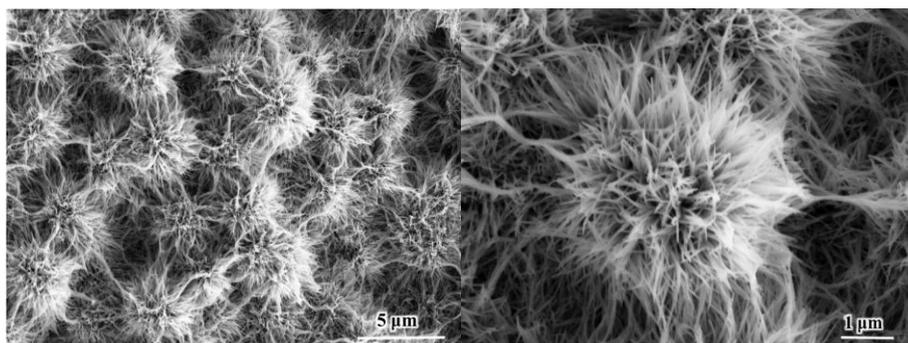
Fig. 1. SEM images of (a)low magnification and (b) high magnification of cluster-like ZnO@Co$_3$O$_4$.
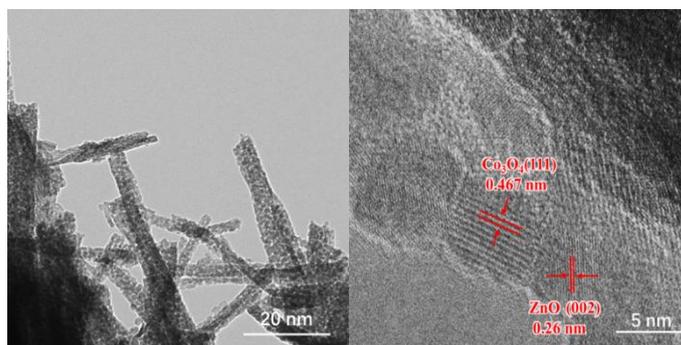
Fig. 2. (a)TEM images and (b) HRTEM images of cluster-like ZnO@Co$_3$O$_4$.

TEM in Figure 2 studies provide insights into cluster like ZnO@Co$_3$O$_4$. For further understanding of the structure, it can be seen that the nanowires of the cluster-like ZnO@Co$_3$O$_4$ are composed of a large number of nanoparticles. The low magnification TEM image in Fig. 2a shows that the nanowire has a diameter of an average size of about 20 nm and is highly porous. It is composed of many nanoparticles with an average size of about 4-6 nm, and the nanowires form clusters through guided self-assembly. The HRTEM image of cluster-like ZnO@Co$_3$O$_4$ of the selected areas in Fig. 2a are shown in Fig. 2b. The lattice spacing of 0.467 nm observed is well corresponded to the (1 1 1) planes of the spinel Co$_3$O$_4$[18]. The lattice spacing of 0.26 nm is agreed with the (0 0 2) lattice planes of hexagonal ZnO structure, which further indicates that the ZnO/Co$_3$O$_4$ composites were successfully synthesized.
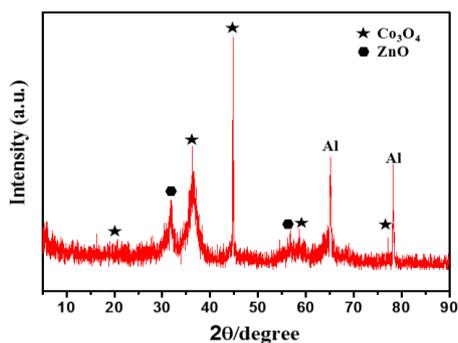
Fig. 3. XRD pattern of cluster-like ZnO@Co$_3$O$_4$.

The XRD pattern of cluster-like $ZnO@Co_3O_4$ in Fig. 3 is used to confirm its phase composition. Referring to the X-ray diffract grams for ZC-3 in Fig. 3, in addition to the peaks from the Al substrate, the diffraction peaks from the cubic Co_3O_4 system are observed [19]. The diffraction peaks from hexagonal wurtzite ZnO are also observed [20], confirm that the product is composed of ZnO and Co_3O_4. It is observed that all ZnO and Co_3O_4 diffraction peaks can be clearly observed and well matched with JCPDS card no. 05-0664 and no. 09-0418, which confirms the formation of ZnO and Co_3O_4 [21].
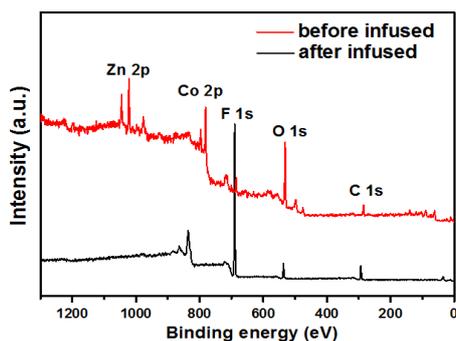
Fig. 4. XPS spectra of before and after infused lubricant oil.

In order to build a thermodynamically stable slip, the following three criteria should be met: (1) the impregnated lubricant (liquid A) should be immiscible without chemical reaction between the substrate and the excluded liquid (liquid B); (2) The matrix shall be wetted preferentially by the injected liquid a rather than liquid B; (3) The matrix shall be rough, porous or swellable in the lubricant [22]. After successfully prepared cluster-like $ZnO@Co_3O_4$ the structure was perfluorinated, and was filled with lubricating oil to obtain SLIPS. The chemical compositions of cluster-like $ZnO@Co_3O_4$ and SLIPS were analyzed by XPS. The survey before and after pouring oil are shown in Fig. 4. Fluorinated cluster-like $ZnO@ Co_3O_4$ have Zn, Co, F, O and C elements, and the peak value of the Zn, Co, O elements decreases and the content of F increases greatly, which proves that the lubricating fluid is filled into the structure and the surface has a certain thickness, masking the cluster-like $ZnO@ Co_3O_4$ structure. This super slippery surface replaces the traditional solid-liquid interface represented by lotus-leaf with liquid-liquid interface, and overcomes the defects of ordinary super hydrophobic surface, such as non-pressure resistance, easy to be infiltrated by liquid with low surface energy and poor stability.

Fig. 5. Sliding behavior of droplets on SLIPS (a) 0s (b) 1s.

Hao et al. proposed that the dynamic behaviour of a droplet on a slippery surface is related to the amount of lubricant on its surface, the thicker the lubricant film is, the faster the droplet slides [23]. The sliding behaviour of water droplets on the slippery cluster-like $ZnO@Co_3O_4$ surface is shown in Fig. 5. After inclining the surface at about 2°, the water droplets can easily slide off, the sliding speed is 2mm/s, indicating the successful construction of SLIPS with cluster-like $ZnO@Co_3O_4$.
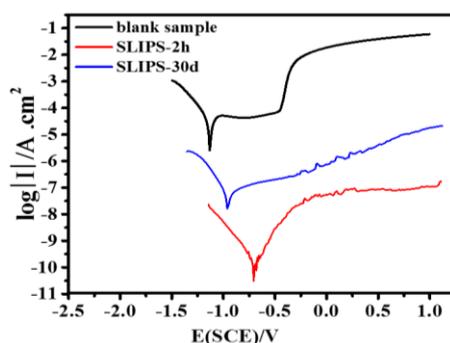
Fig. 6. Polarization curves of different samples immersed in 3.5 wt% NaCl solution.

In a traditional three electrode system, the corrosion medium was 3.5% NaCl solution of simulated seawater. The corrosion resistance of the samples was studied by potentiodynamic polarization (IE) experiment and electrochemical impedance spectroscopy (EIS). Fig. 6 shows the polarization curves of blank sample, SLIPS after immersion in 3.5 wt.% NaCl solution for 2 h and 30 d. The relevant electrochemical parameters obtained from the test are summarized in Table 2. The passivation of aluminum alloy can help to reduce corrosion process [24], but the high polarization current density (icorr) shows that the blank sample is still easily prone to corrode in the presence of chloride ions. Both polarization current densities of SLIPS-2h and SLIPS-30d much lower than that of blank sample. The i_{corr} of SLIPS-2h is 6 orders of magnitude lower than that of blank sample, and the i_{corr} of SLIPS-30d is also 4 orders of magnitude lower than that of blank sample. The results show that SLIPS has high corrosion resistance even after soaking for 30 days. Moreover, there is no passivation region in the polarization curves of SLIPS-2h and SLIPS-30d, which proved that SLIPS are insensitive to a pitting corrosion. Namely, SLIPS can inhibit the corrosion of underlying substrate and present advantage in maintaining stability in corrosive medium. In addition, β_a can be used to reflect the difficulty and slope of electrode reaction. The greater the β_a, the greater the resistance to the anode reaction of the electrode, and the lower the activation performance of the aluminum alloy. Compared with untreated aluminum alloy, β_a increases to a certain extent, and the polarization curve of the super sliding surface becomes not as smooth as the blank sample, indicating that the liquid injection changes the properties of the solution/metal interface, effectively inhibits the activity of the alloy substrate and improves the corrosion resistance.

Table 2. The electrochemical parameters for polarization.

Samples	E_{corr} (V)	I_{corr} (A/cm^2)
Blank sample	-1.232	1.33×10^{-4}
SLIPS-2h	-0.703	9.28×10^{-9}
SLIPS-30d	-0.951	3.57×10^{-7}
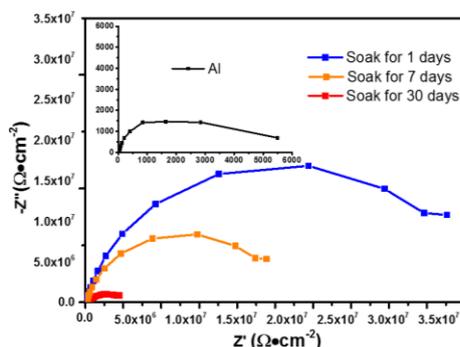
Fig. 7. EIS results of SLIPS based on cluster-like ZnO@Co$_3$O$_4$ after immersion in a 5% NaCl solution for different times.

In order to further characterize the corrosion resistance, the corrosion resistance of the samples was analyzed by electrochemical impedance spectroscopy. Figure 7 shows the Nyquist diagram of blank samples and SLIPS soaked for 1d, 7d and 30d. As can be seen from the inset in Figure 7, the impedance radius of untreated aluminum alloy is only 6000 ohms. According to the previous study [25-27], the larger the radius of capacitive reactance arc in Nyquist diagram, the better the corrosion resistance of working electrode. At room temperature, the Nyquist diagram of slides samples immersed in NaCl solution for different times can be seen that the longer the immersion time is, the radius of capacitive resistance arc gradually decreases, indicating that the corrosion resistance of the prepared samples is weakened, but it is still higher than that of blank aluminum alloy. It also can be seen from the Nyquist diagram that the radius of the impedance circle after 1d in 3.5wt% NaCl solution is very large. With the increase of immersion time, the radius of the impedance circle decreases, indicating that the coating is attacked by Cl$^-$ in the solution. In the 30 days of immersion, there has been no Warburg impedance in the low frequency range, which shows that the SLIPS can effectively prevent the corrosion of the alloy substrate. At the initial stage of immersion, the impedance arc radius can reach 10^7 $\Omega \cdot$cm^2. It is worth considering that after soaking for 30 days, the |Z| value of SLIPS sample is about 10^6 $\Omega \cdot$ cm^2, which is about 4 orders of magnitude higher than that of untreated sample (10^3 $\Omega \cdot$ cm^2). The above results are consistent with the results of potentiodynamic polarization curve, indicating that the injected lubricating fluid does not disappear and effectively improves the corrosion resistance of aluminum alloy substrate.
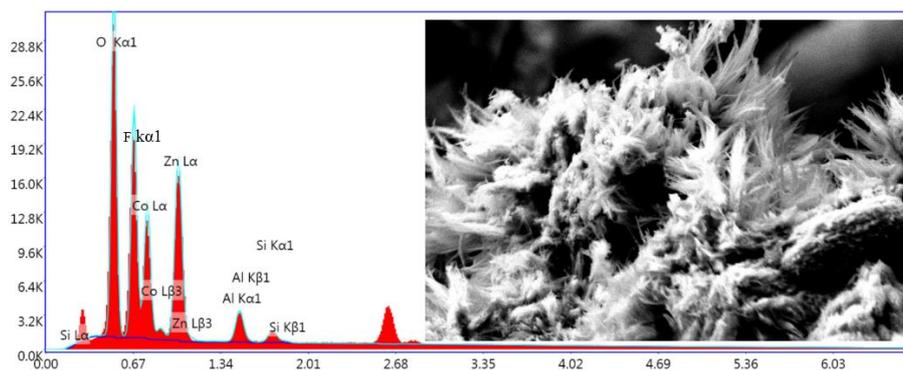
Fig. 8. SEM and EDS images of SLIPS based on cluster-like ZnO@Co$_3$O$_4$ after 30 d immersion.

Surface analysis data of SLIPS based on cluster-like ZnO@Co$_3$O$_4$ shows in the Fig.8. It can be seen from the SEM image that the cluster structure has almost no change, the complete nanowire structure can still be seen, and some corrosion products were deposited on the surface. From the perspective of elemental analysis, although it has been soaked for 30 days, the content of F is very high, which can maintain the hydrophobic characteristics and still provide effective protection measures for the substrate.

4. Conclusions

A clusters-like ZnO@Co$_3$O$_4$ structure were constructed on aluminum alloy substrate by a hydrothermal method. A new type of super slippery surface was successfully prepared by filling lubricating fluid after fluorination modification. The ZnO@Co$_3$O$_4$ structure effectively improves the storage capacity of lubricating fluid. The self-corrosion current density of this surface is 9.28×10^{-9} A/cm^2, about 6 orders of magnitude lower than the untreated aluminum alloy substrate. At the beginning of immersion, the low-frequency impedance modulus ($|Z|_{0.01Hz}$) is as high as 10^7 $\Omega \cdot$ cm^2. After soaking in 3.5% NaCl solution of simulated seawater for 30 days, the low-frequency impedance modulus is about 5.0×10^6 $\Omega \cdot$ cm^2, 3 orders of magnitude higher than the blank sample at the beginning of soaking

Acknowledgements

References

[1] Y. N. Lin, H. Y. Wu, G. Z. Zhou, C. H. Chiu, S. Lee, Mater. Des. **29**, 2061 (2008).
[2] S. Katsikis, B. Noble, S. J. Harris, Mater. Sci. Eng. A **485**, 613 (2008).
[3] N. Yamauchi, N. Ueda, A. Okamoto, T. Sone, M. Tsujikawa, S. Oki, Surf. Coat. Tech. **201**,

4913 (2007).

[4] K. Terpilowski, D. Rymuszka, L. Hołysz, M. Ilnicki, Surf. Interface Anal. **49**, 647 (2017).

[5] A. Z. Zhuk, A. E. Sheindlin, B. V. Kleymenov, E. I. Shkolnikov, M. Y. Lopatin, J. Power Sources **157**, 921 (2006).

[6] S. J. Yang, S. L. Dai, Mater. Rev. **2**, 022 (2005).

[7] H. X. Li, Q. L. Bai, Y. Li, Q. Du, L. Katgerman, J. S. Zhang, L. Z. Zhuang, Mater. Sci. Eng. A **698**, 230 (2017).

[8] Yuki Otani, Shinya Sasaki, Mater. Sci. Eng. A **777**, 139079 (2020).

[9] X. Yu, M. Zhao, R. Li, J. Wang, Dig J Nanomater Bios **16**, 685 (2021).

[10] H. Ezuber, A. El-Houd, F. El-Shawesh, Mater. Des. **29**, 801 (2008).

[11] M. Meikandan, K. M. Mohan, R. Velraj, Dig J Nanomater Bios **11**, 945 (2016).

[12] Y. A. Kuzenkov, S. V. Oleinik, A. S. Zimina et al., Prot Met Phys Chem Surf. **52**, 1175 (2016).

[13] D. Gasco-Owens, V. Veys-Renaux, E. Cartigny, E. Rocca, Electrochimica Acta **382**, 138303 (2021).

[14] Y. Zhu, J. C. Zhang, Y. M. Zheng et al., Adv. Funct. Mater. **16**, 568 (2006).

[15] W. Barthlott, C. Neinhuis, Planta **202**, 1 (1997).

[16] K. Golovin, D. H. Lee, J. M. Mabry, A. Tuteja, Angew. Chem. Int. Ed. **52**, 13007 (2013).

[17] T. S. Wong, S. H. Kang, S. K. Tang, E. J. Smythe, B. D. Hatton, A. Grinthal, J. Aizenberg, Nature **477**, 443 (2011).

[18] L Zhang, X Jing, J Liu, J Wang, Y Sun, Sensors and Actuators B **221**, 1492 (2015).

[19] T. Zhu, J. S. Chen, W. L. Xiong, J. Mater. Chem. **20**, 7015 (2010).

[20] G. R. Li, Z. L. Wang, F. L. Zheng, Y. N. Ou, Y. X. Tong, J. Mater. Chem. **21**, 4217 (2011).

[21] M. Zhang, J. Yu, J. Wang, Surf. Coat. Tech. **407**, 126772 (2021).

[22] A. Barba, A. Diezescudero, Y. Maazouz, ACS Appl. Mater. Interfaces **48**, 41722 (2017).

[23] C. Hao, J. Li, Y. Liu, X. Zhou, Y. Liu, R. Liu, L. Che, W. Zhou, D. Sun, L. Li, Nat. Commun. **6**, 7986 (2015).

[24] M. Zhang, Q. Liu, R. Chen, H. Chen, D. Song, J. Liu, H. Zhang, R. Li, Y. Wang, J. Wang, J. Alloys Compd. **764**, 730 (2018).

[25] H. Y. Ma, C. Yang, S. H. Chen, L. Y. Jiao, X. S. Huang, Electrochim. Acta **48**, 4277 (2003).

[26] H. P. Ji, J. M. Park, Surf. Coat. Technol. **254**, 167 (2014).

[27] C. Jeong, J. Lee, K. Sheppard, C. H. Choi, Langmuir **31**, 11040 (2015).